



C₅ glycolipids of heterocystous cyanobacteria track symbiont abundance in the diatom *Hemiaulus hauckii* across the tropical North Atlantic

Nicole J. Bale¹, Tracy A. Villareal², Ellen C. Hopmans¹, Corina P. D. Brussaard¹, Marc Besseling¹, Denise Dorhout¹, Jaap S. Sinninghe Damsté^{1,3}, and Stefan Schouten^{1,3}

¹Department of Marine Microbiology and Biogeochemistry, NIOZ Royal Institute for Sea Research, and Utrecht University, P.O. Box 59, 1790 AB Den Burg, the Netherlands

²Marine Science Institute, The University of Texas at Austin, Port Aransas, TX, USA

³Utrecht University, Faculty of Geosciences, Department of Earth Sciences, P.O. Box 80.021, 3508 TA Utrecht, the Netherlands

Correspondence: Nicole J. Bale (nicole.bale@nioz.nl)

Received: 14 July 2017 – Discussion started: 23 August 2017

Revised: 19 December 2017 – Accepted: 3 January 2018 – Published: 1 March 2018

Abstract. Diatom–diazotroph associations (DDAs) include marine heterocystous cyanobacteria found as exosymbionts and endosymbionts in multiple diatom species. Heterocysts are the site of N₂ fixation and have thickened cell walls containing unique heterocyst glycolipids which maintain a low oxygen environment within the heterocyst. The endosymbiotic cyanobacterium *Richelia intracellularis* found in species of the diatom genus *Hemiaulus* and *Rhizosolenia* makes heterocyst glycolipids (HGs) which are composed of C₃₀ and C₃₂ diols and triols with pentose (C₅) moieties that are distinct from limnetic cyanobacterial HGs with predominantly hexose (C₆) moieties. Here we applied a method for analysis of intact polar lipids to the study of HGs in suspended particulate matter (SPM) and surface sediment from across the tropical North Atlantic. The study focused on the Amazon plume region, where DDAs are documented to form extensive surface blooms, in order to examine the utility of C₅ HGs as markers for DDAs as well as their transportation to underlying sediments. C₃₀ and C₃₂ triols with C₅ pentose moieties were detected in both marine SPM and surface sediments. We found a significant correlation between the water column concentration of these long-chain C₅ HGs and DDA symbiont counts. In particular, the concentrations of both the C₅ HGs (1-(O-ribose)-3,27,29-triacontanetriol (C₅ HG₃₀ triol) and 1-(O-ribose)-3,29,31-dotriacontanetriol (C₅ HG₃₂ triol)) in SPM exhibited a significant correlation with the number of *Hemiaulus hauckii* symbionts. This result strengthens the

idea that long-chain C₅ HGs can be applied as biomarkers for marine endosymbiotic heterocystous cyanobacteria. The presence of the same C₅ HGs in surface sediment provides evidence that they are effectively transported to the sediment and hence have potential as biomarkers for studies of the contribution of DDAs to the paleo-marine N cycle.

1 Introduction

Cyanobacteria are cosmopolitan oxygenic photoautotrophs that play an important role in the global carbon and nitrogen cycles. Marine cyanobacteria are the major fixers of dinitrogen (N₂) in modern tropical and subtropical oligotrophic oceans (Karl et al., 1997; Lee et al., 2002). Because N₂ fixation is sensitive to oxygen, cyanobacteria have evolved a range of different strategies in order to combine the incompatible processes of oxygenic photosynthesis and N₂ fixation. One strategy, found only in filamentous cyanobacteria, is to fix N₂ in differentiated cells known as heterocysts (Wolk, 1973; Rippka et al., 1979). Free-living heterocystous cyanobacteria are rare in the open ocean (Staal et al., 2003); however, heterocystous taxa are abundant as both exosymbionts and endosymbionts in diatoms (Foster et al., 2011; Gómez et al., 2005; Luo et al., 2012; Villareal, 1991; Villareal et al., 2011, 2012). These diatom–diazotroph associa-

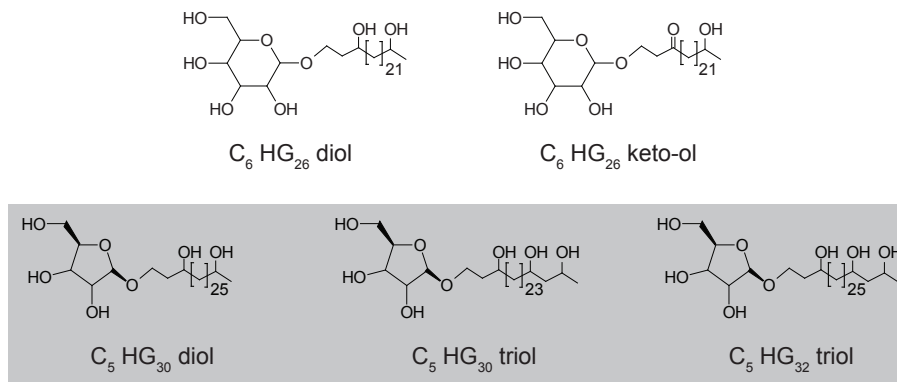


Figure 1. Structures of the heterocyst glycolipids detected in this study. C₆ glycolipids: 1-(O-hexose)-3,25-hexacosanediol (C₆ HG₂₆ diol), 1-(O-hexose)-3-keto-25-hexacosanol (C₆ HG₂₆ keto-ol). C₅ glycolipids: 1-(O-ribose)-3,29-triacontanediol (C₅ HG₃₀ diol), 1-(O-ribose)-3,27,29-triacontanetriol (C₅ HG₃₀ triol), 1-(O-ribose)-3,29,32-dotriacontanetriol (C₅ HG₃₂ triol). Grey box indicates glycolipids associated with DDAs.

tions (DDAs) can fully support the nitrogen (N) requirements of both host and symbiont (Foster et al., 2011; Villareal, 1990) which explains the presence of these symbioses in oligotrophic offshore environments such as the North Pacific Gyre (Venrick, 1974). In the western tropical North Atlantic Ocean, these symbiotic associations produce nearly 70 % of total N demand in the surface waters (Carpenter et al., 1999) as non-symbiotic diatom blooms deplete N in the Amazon River plume and create N-poor conditions with residual P and Si (Subramaniam et al., 2008; Weber et al., 2017).

In all heterocystous non-symbiotic cyanobacteria studied to date, the heterocyst cell walls contain heterocyst glycolipids (HGs; Abreu-Grobois et al., 1977; Bauersachs et al., 2009a, 2014; Gambacorta et al., 1995; Nichols and Wood, 1968). These HGs almost universally comprise a hexose head group (C₆) glycosidically bound to long-chain diols, triols or hydroxyketones (see Fig. 1; Bauersachs et al., 2009b, 2011; Bryce et al., 1972; Gambacorta et al., 1998). In contrast, the endosymbiotic heterocystous cyanobacterium *Richelia intracellularis* (found within the marine diatoms *Hemiaulus hauckii* and *H. membranaceus*; Villareal, 1991) contained C₃₀ and C₃₂ diol and triol HGs with a pentose sugar head group (C₅), identified as D-ribose, rather than a C₆ sugar (Fig. 1; Schouten et al., 2013). The structural difference in the glycolipids of marine endosymbiotic heterocystous cyanobacteria compared to the free-living counterparts was hypothesized to be an adaptation to the high intracellular O₂ concentrations within the host diatom (Schouten et al., 2013).

In the first study of the C₃₀ and C₃₂ diol and triol C₅ HGs in the natural environment, these compounds were found in suspended particulate material (SPM) and surface sediment from the Amazon plume but not in lake sediments or river SPM (Bale et al., 2015). HGs with a C₅ sugar moiety comprising a shorter C₂₆ carbon chain (hereafter called short-chain C₅ HGs) were tentatively identified in a culture of freshwater cyanobacterium *Aphanizomenon ovalisporum*

UAM 290 and in suspended particulate matter from three freshwater environments in Spain (Wörmer et al., 2012). Thus, it remains to be demonstrated whether C₃₀ and C₃₂ diol and triol C₅ HGs (hereafter called long-chain C₅ HGs) are unambiguously associated with DDAs in the marine environment. In addition, the genera *Rhizosolenia*, *Guinardia* and *Hemiaulus* all contain species harboring heterocystous cyanobacteria. DDA taxonomic relationships and host-symbiont specificity are only partially defined (Hilton, 2014; Foster and Zehr, 2006; Janson et al., 1999), suggesting additional clarification of how diverse HGs are distributed within DDAs is required.

In this study, we applied a novel method coupling ultra-high-pressure liquid chromatography with high-resolution mass spectrometry (UHPLC-HRMS) method to analyze the concentration of HG lipids in SPM from the oligotrophic open Atlantic Ocean to the region affected by the Amazon River plume. We compared lipid concentrations with the number of diazotrophic symbionts to examine the applicability of HGs to trace these organisms. Furthermore, we also analyzed HG lipids in the surface sediment along the transect to examine the transport of these compounds to the geological record and potential for use as a molecular tracer for DDA N₂ fixation.

2 Methods

2.1 Cruise track and physicochemical parameters

Sampling was carried out during a 4-week research cruise (64PE393) onboard the R/V *Pelagia* from 26 August to 21 September 2014. The cruise followed a > 5000 km transect and sampling occurred at 23 stations, starting at Cabo Verde and finishing at the island of Barbados (Fig. 2). The cruise track began close to the Cabo Verde exclusive economic zone boundary and proceeded approximately south-

Table 1. Glycolipid concentrations from sea surface (3–5 m) and surface sediment for all stations. For concentrations at bottom wind mixed layer (BWML) and deep Chl maximum (DCM) see Table S3.

Station	Lat.	Long.	Date	Water depth (m)	Sea surface			Surface sediment		
					Salinity	C ₅ HG ₃₀ triol (pgL ⁻¹)	C ₅ HG ₃₂ triol (pgL ⁻¹)	C ₅ HG ₃₀ triol (ng g ⁻¹)	C ₅ HG ₃₂ triol (ng g ⁻¹)	TOC (%)
1	15.02	-30.56	29 Aug 2014	5500	36.4	18	0	1.7 ± 0.4	0.2 ± 0.1	0.6 ± 0.0
2*	14.35	-32.58	30 Aug 2014	6300	36.5	ns	ns	*	*	*
3	13.16	-36.21	31 Aug 2014	5190	36.4	24.6	0	3.3 ± 0.8	0.4 ± 0.1	0.6 ± 0.0
4*	12.41	-38.50	01 Sep 2014	4810	36.2	40.9	0	*	*	*
5	10.83	-40.47	02 Sep 2014	4620	36	8.9	0	2.3 ± 0.9	0.3 ± 0.1	0.5 ± 0.1
6*	9.41	-42.10	03 Sep 2014	3610	36.1	27.3	0	*	*	*
7	7.52	-44.28	04 Sep 2014	4650	33.5	773	66.2	14.6 ± 6.8	1.7 ± 1.0	0.7 ± 0.0
8	6.49	-45.45	05 Sep 2014	4250	31.9	4837	469	9.7 ± 1.7	1.0 ± 0.1	0.6 ± 0.0
9	5.60	-46.40	06 Sep 2014	3770	32.2	24.6	0	4.8 ± 0.6	0.4 ± 0.0	0.5 ± 0.0
10	6.68	-47.49	07 Sep 2014	4080	31.3	13.3	0	6.8 ± 4.4	0.7 ± 0.2	0.7 ± 0.0
11	5.53	-51.50	10 Sep 2014	80	29.2	0	0	0.2 ± 0.1	0.01 ± 0.01	0.1 ± 0.0
12	6.07	-52.46	10 Sep 2014	70	35.4	3.01	0	0.3 ± 0.1	0.01 ± 0.01	0.3 ± 0.1
13	7.60	-53.02	11 Sep 2014	1000	32.8	31.1	0	7.4 ± 3.0	0.9 ± 0.4	1.2 ± 0.0
14	9.53	-51.32	12 Sep 2014	4840	31.4	316	6.2	13.5 ± 1.4	1.3 ± 0.2	0.9 ± 0.0
15*	8.95	-49.98	13 Sep 2014	4660	32.7	565	24.4	*	*	*
16	10.22	-51.88	14 Sep 2014	4940	33.9	391	27.3	13.0 ± 6.1	1.6 ± 0.5	1.0 ± 0.1
17	9.90	-53.27	15 Sep 2014	4750	31.6	379	15.5	9.4 ± 3.0	0.9 ± 0.3	0.9 ± 0.1
18*	9.37	-55.20	16 Sep 2014	3590	33.2	611	67.2	*	*	*
19*	10.52	-55.48	16 Sep 2014	4180	32.8	390	34.5	*	*	*
20a	11.27	-54.16	17 Sep 2014	4790	33.9	2.3	0	17.6 ± 7.0	1.4 ± 1.2	0.8 ± 0.0
20b*	11.47	-54.21	17 Sep 2014	4830	34.2	67.7	0	*	*	*
21a	13.02	-54.67	18 Sep 2014	5040	33.8	196	9.8	12.9 ± 1.7	1.6 ± 0.1	0.6 ± 0.0
21b*	13.20	-54.72	18 Sep 2014	5170	34.8	249	6.5	*	*	*
22	14.80	-55.18	19 Sep 2014	5500	35.6	48.6	0.4	13.4 ± 4.5	2.4 ± 1.1	0.7 ± 0.1
23	15.79	-57.05	20 Sep 2014	5320	34	106	5.9	9.8 ± 3.5	1.4 ± 0.5	0.6 ± 0.0

* No sediment collected. ns: not sampled.

westerly across the Atlantic (Fig. 2). Aquarius sea-surface salinity (SSS) satellite data (30-day composite, centered on 1 September 2014) clearly indicated the influence of the freshwater Amazon discharge in the region, i.e., surface salinity < 33 (Fig. 2). Discrete CTD measurements of salinity (contour lines Fig. 3a, Table 1) generally agreed with the satellite data as to the geographical spread of the Amazon River plume. However, the region was highly dynamic with the plume location shifting hundreds of km over the course of the cruise as noted in the sequential 7-day Aquarius SSS composites (Fig. S1 in the Supplement).

Temperature and salinity were measured using a Sea-Bird SBE911+ conductivity–temperature–depth (CTD) system equipped with a 24 × 12 L Niskin bottle rosette sampler. Fluorescence was measured with a Chelsea Aquatracka MKIII fluorometer. Chlorophyll fluorescence was not calibrated against discrete chlorophyll and is reported as relative fluorescence units (RFU). Seawater samples for dissolved inorganic nutrient analysis were taken from the Niskin bottles in 60 mL high-density polyethylene syringes with a three-way valve and filtered over Acrodisc PF syringe filters (0.8/0.2 µm Supor Membrane, PALL Corporation) into pre-rinsed 5 mL polyethylene vial. Dissolved orthophosphate (PO₄³⁻) and nitrogen (NO₃⁻, NO₂ and NH₄⁺) were stored in dark at 4 °C until analysis onboard (within 18 h) using a QuAAtro auto-

analyzer (Grasshoff, 1983; Murphy and Riley, 1962). Samples for dissolved reactive silicate (Si) analysis (Strickland and Parsons, 1968) were stored dark at 4 °C until analysis using the same system as above upon return to the Royal Netherlands Institute for Sea Research (NIOZ). The detection limits were calculated as PO₄³⁻ 0.004 µmol L⁻¹, NH₄⁺ 0.030 µmol L⁻¹, NO₃⁻ + NO₂ 0.005 µmol L⁻¹ and NO₂ 0.002 µmol L⁻¹.

2.2 Phytoplankton pigment composition and enumeration of diazotrophs

Samples for diazotroph enumeration were collected in polycarbonate bottles of which 500–1170 mL was filtered under gentle vacuum (< 5 psi) through a 10 µm pore-size polycarbonate filter (47 mm diameter). Filters were placed onto 75 × 50 mm glass slides (Corning 2947) and 2–3 drops of non-fluorescent immersion oil (Cargille-type DF) placed on the slide. A glass cover slip (45 × 50 mm; Fisherbrand 12-545-14) was placed on the filter sample and allowed to sit while the immersion oil cleared the filter. The sample was subsequently viewed under transmitted light and epifluorescence illumination light filter (530–560 nm excitation, 572–648 nm emission; Olympus BX51) for counting/identifying

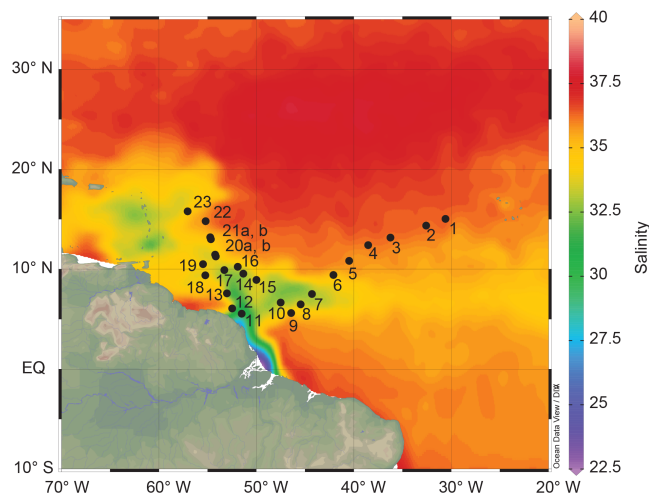


Figure 2. Map of tropical North Atlantic showing the study site. Location of the stations indicated. Aquarius sea-surface salinity (SSS) satellite data from ERDAPP (30-day composite, centered on 1 September 2014, <https://coastwatch.pfeg.noaa.gov/erdapp/index.html>).

trichomes and host cells as well as photomicrography (Olympus DP70).

For phytoplankton pigment analysis, seawater was filtered through 0.7 μm glass fiber GF/F filters (Pall Corporation, Port Washington, NY). The filters were extracted in 4 mL 100 % methanol buffered with 0.5 mol L^{-1} ammonium acetate, homogenized for 15 s and analyzed by high-performance liquid chromatography (HPLC). The relative abundances of the different taxonomic groups were determined using CHEMTAX (Mackey et al., 1996; Riegman and Kraay, 2001).

2.3 SPM and surface sediment collection

Three McLane in situ pumps (McLane Laboratories Inc., Falmouth) were used to collect suspended particulate matter (SPM) from the water column for lipid analysis. They were generally deployed at three depths: the surface (3–5 m), the bottom wind mixed layer (BWML) and the deep chlorophyll-*a* maximum (DCM), with some additional sampling at 200 m (Table 1). They pumped between 90 and 380 L with a cut-off at a pre-programmed pressure threshold and the SPM was collected on pre-ashed 0.7 $\mu\text{m} \times 142 \text{ mm}$, GF/F filters (Pall Corporation, Port Washington, NY) and immediately frozen at -80°C . At Station 10, as part of a different study (Besseling et al., 2018), 12 additional sampling points were carried out to produce a high-resolution depth profile (Table 2) where the SPM was collected on pre-ashed 0.3 μm GF75 filters (Avantec, Japan).

Sediment was collected at each station in 10 cm diameter, 60 cm length multicores. For each sediment sampling site, triplicate cores were collected, always from a single multicore deployment (with a maximum of 60 cm between core

centers). The cores were sliced into 1 cm slices using a hydraulic slicer and each slice was stored separately in a geochemical bag and immediately frozen at -80°C . For this study, we analyzed the 0–1 cm (surface sediment) slice. For analysis of the content of total organic carbon (TOC), sediment was freeze dried, decalcified in silver cups with 2 M HCl and analysis was carried out using a Flash 2000 series elemental analyzer (Thermo Scientific) equipped with a TCD detector.

2.4 Lipid extraction

The extraction of lipids from freeze dried filters or sediment samples was carried out using a modified Bligh–Dyer extraction (Bale et al., 2013). The samples were extracted in an ultrasonic bath for 10 min with 5–20 mL of single-phase solvent mixture of methanol (MeOH):dichloromethane (DCM): phosphate buffer (2 : 1 : 0.8, $v/v/v$). After centrifugation ($1000 \times g$ for 5 min, room temperature, Froilabo Fir-labo SW12 with swing-out rotor) to separate the solvent extract and residue, the solvent mixture was collected in a separate flask. This was repeated three times before DCM and phosphate buffer were added to the single-phase extract to induce phase separation, producing a new ratio of MeOH:DCM: phosphate buffer (1 : 1 : 0.9 $v/v/v$). After centrifugation ($1000 \times g$ for 5 min), the DCM phase was collected in a glass round-bottom flask and the remaining MeOH: phosphate buffer phase was washed two additional times with DCM. Rotary evaporation was used to reduce the combined DCM phase before it was evaporated to dryness under a stream of N_2 .

2.5 Analysis of intact polar lipids

Whereas previous studies of heterocyst glycolipids have applied high-performance liquid chromatography multiple reaction monitoring (MRM) mass spectrometry (HPLC–MS²) method (e.g., Bale et al., 2015), in this study we used an UHPLC–HRMS method, designed for the analysis of a wide range of intact polar lipids (Moore et al., 2013). The UHPLC–HRMS method was adapted by replacement of hexane with heptane as the non-polar solvent in the eluent, to reduce the toxic nature of hexane relative to heptane in terms of the workplace health hazard (Buddrick et al., 2013; Carelli et al., 2007; Daughtrey et al., 1999). Our UHPLC–HRMS method was as follows: we used an Ultimate 3000 RS UHPLC, equipped with thermostatted auto-injector and column oven, coupled to a Q Exactive Orbitrap MS with Ion Max source with a heated electrospray ionization (HESI) probe (Thermo Fisher Scientific, Waltham, MA). Separation was achieved on a YMC-Triart Diol-HILIC column (250 \times 2.0 mm, 1.9 μm particles, pore size 12 nm; YMC Co., Ltd, Kyoto, Japan) maintained at 30 $^\circ\text{C}$. Elution was achieved with (A) heptane/propanol/formic acid/14.8 mol L^{-1} aqueous NH_3 (79 : 20 : 0.12 : 0.04, $v/v/v/v$) and (B) propanol

Table 2. The additional SPM samples collected for high-resolution depth profile at Station 10 (0.3 µm GF75 filters).

Sampling depth (m)	Salinity	Temperature (°C)	C ₅ HG ₃₀ triol (pgL ⁻¹)	C ₅ HG ₃₂ triol (pgL ⁻¹)	Sum (pgL ⁻¹)
20	35.3	28.6	5.6	0.0	5.6
50*	36.4	27.3	9.6	0.0	9.6
200	35.2	11.4	108	0.3	108
400	34.7	7.4	24.4	0.1	24.5
600	34.6	6.3	29.0	0.1	29.1
800	34.6	5.1	22.5	0.4	22.9
1000	34.7	4.7	11.9	0.2	12.2
1200	34.8	4.8	12.6	0.2	12.8
1500	35.0	4.5	16.2	0.3	16.5
2000	35.0	3.4	18.3	0.3	18.6
2500	34.9	2.8	20.7	0.4	21.0
3000	34.9	2.4	22.3	0.3	22.6

* Deep chlorophyll maximum.

water/formic acid/14.8 molL⁻¹ aqueous NH₃ (88 : 10 : 0.12 : 0.04, *v/v/v/v*) starting at 100 % A, followed by a linear increase to 30 % B at 20 min, followed by a 15 min hold and a further increase to 60 % B at 50 min. Flow rate was 0.2 mL min⁻¹, total run time was 70 min, followed by a 20 min re-equilibration period. Positive ion ESI settings were capillary temperature, 275 °C; sheath gas (N₂) pressure, 35 arbitrary units (AU); auxiliary gas (N₂) pressure, 10 AU; spray voltage, 4.0 kV; probe heater temperature, 275 °C; S-lens 50 V. Target lipids were analyzed with a mass range of *m/z* 350–2000 (resolution 70 000 ppm at *m/z* 200), followed by data-dependent tandem MS² (resolution 17 500 ppm), in which the 10 most abundant masses in the mass spectrum were fragmented successively (normalized collision energy, 35; isolation width, 1.0 *m/z*). The Q Exactive was calibrated within a mass accuracy range of 1 ppm using the Thermo Scientific Pierce LTQ Velos ESI Positive Ion Calibration Solution. During analysis, dynamic exclusion was used to temporarily exclude masses (for 6 s) in order to allow selection of less abundant ions for MS². In addition, an inclusion list (within 3 ppm) was used, containing all known HGs, in order to obtain confirmatory fragment spectra.

Before analysis, the extracts were re-dissolved in a mixture of heptane, isopropanol and water (72 : 27 : 1, *v/v/v*) which contained two internal standards (IS), a platelet-activating factor (PAF) standard (1-O-hexadecyl-2-acetyl-sn-glycero-3-phosphocholine, 5 ng on column) and a C₁₂ alkyl chain glycolipid standard, *n*-dodecyl-β-D-glucopyranoside (≥ 98 % Sigma-Aldrich, 20 ng on column; see Bale et al., 2017). The samples were then filtered through 0.45 µm mesh true regenerated cellulose syringe filters (4 mm diameter; Grace Alltech).

The injection volume was 10 µL for each sample. For quantification the relative response factor (RRF) between the *n*-dodecyl-β-D-glucopyranoside IS and an isolated C₆ HG (1-(O-hexose)-3,25-hexacosanediol (Bale et al., 2017) was

determined to be 6.63. It is not currently possible to isolate enough of a naturally occurring pentose glycolipid due to the limitations of culturing sufficient diatom–diazotroph biomass. As we do not expect significant differences in ionization efficiency between a hexose and a pentose glycolipid, we assume that the RRF of the internal standard and the hexacosanediol C₆ HG is similar to that of C₅ HGs. Nevertheless, quantification of the pentose glycolipids should be interpreted with care.

The 12 samples collected at Station 10 (0.3 µm GF75 filters, Table 2) were analyzed on the same UHPLC-HRMS system, but with hexane instead of heptane in the mobile phase. Also, the *n*-dodecyl-β-D-glucopyranoside IS was not added, so quantification was based on the PAF IS and included correction for the RRF between the *n*-dodecyl-β-D-glucopyranoside IS and the PAF IS.

2.6 Statistical analysis

T tests and Pearson correlations were determined using Sigmaplot software (version 13.0). Regression curves were plotted and analyzed in Windows Excel.

3 Results

3.1 Physicochemical conditions and phytoplankton assemblage

Stations 1–6, 12 (close to coast, north of Amazon plume) and 22 correspond to oceanic stations (SSS > 35, following the convention of Subramaniam et al., 2008), with Stations 7–10, 13–21 and 23 in the intermediate salinity range (30–35). Originally termed mesohaline (Subramaniam et al., 2008), we use “intermediate salinity” to avoid confusion with the older use of mesohaline in coastal systems to refer to 5–18 waters (Elliott and McLusky, 2002). Only Sta-

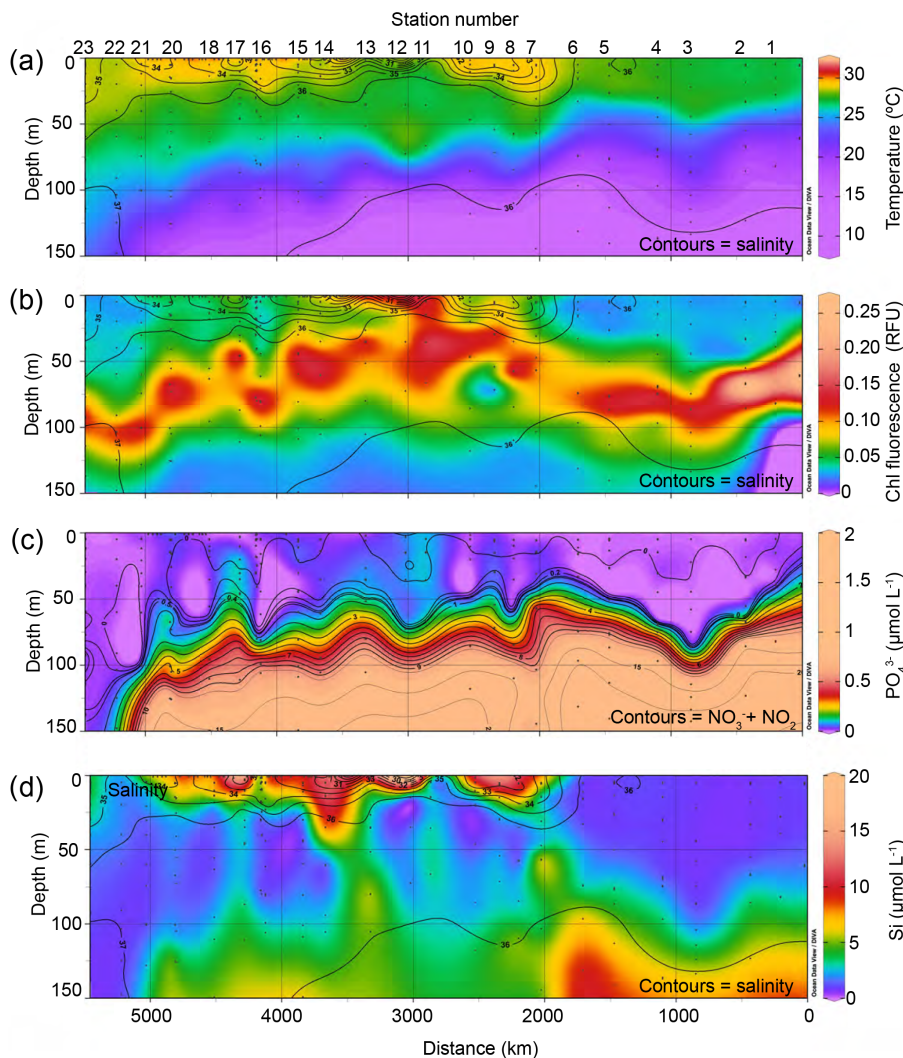


Figure 3. Water column characteristics along the cruise track. Color scales show (a) temperature, (b) chlorophyll fluorescence (from fluorometer on CTD), (c) PO₄³⁻ (color scale) and (d) Si. Contour lines show salinity (a, b, d) and NO₃⁻ + NO₂ (c). Station numbers noted above plots, distance along transect from the Cabo Verde islands below.

tion 11, with an SSS of 29.2, was in the low-salinity range defined by Subramaniam et al. (2008). Temperature was uniformly high across the cruise track ($> 27^{\circ}\text{C}$ in the euphotic zone) with the 25°C isotherm deepening along the cruise track (Fig. 3a). Oceanic Stations 1–6 exhibited depleted surface (3–5 m) inorganic nutrient concentrations (on average $0.01 \pm 0.01 \mu\text{mol L}^{-1}$ PO₄³⁻, $0.02 \pm 0.20 \mu\text{mol L}^{-1}$ NO₃⁻ + NO₂ and $0.86 \pm 0.09 \mu\text{mol L}^{-1}$ Si; Fig. 3c and d). Surface NO₃⁻ + NO₂ and PO₄³⁻ concentration remained low at the subsequent intermediate salinity stations (Stations 7–11; Fig. 3c), while Si concentrations increased > 10 -fold to an average of $12.1 \pm 4.4 \mu\text{mol L}^{-1}$ (Fig. 3d). From the coastal shelf of French Guiana (Stations 11 and 12), the cruise progressed in a northerly direction towards the Caribbean. The Amazon River influence was again evident after Station 13, but decreased with distance, ranging from 32.8 to

a maximum of 35.6 (Station 22). Surface NO₃⁻ + NO₂ remained low at these intermediate salinity stations (on average $0.01 \pm 0.00 \mu\text{mol L}^{-1}$), while PO₄³⁻ was variable but generally decreased to open ocean levels (from $0.01 \mu\text{mol L}^{-1}$ to below the limit of detection) and Si dropped from 10.4 to $3.94 \mu\text{mol L}^{-1}$.

The deep chlorophyll (Chl) maximum (DCM; see maxima in Chl fluorescence, Fig. 3b) was associated with the nutricline (see Fig. 3c) over most of the transect, with the highest DCM fluorescence at the oceanic stations and a secondary surface Chl fluorescence maximum at the low-salinity station (Station 11).

The phytoplankton pigment composition analysis at the oceanic stations (1–6) was dominated by the cyanobacteria *Prochlorococcus*, which made up around 50% of total Chl *a* in the surface waters (Table S1). At the intermedi-

ate salinity stations (7–10 and 18–23), the phycoerythrin-containing cyanobacteria (e.g., *Synechococcus*) dominated the phytoplankton community. In general, at Stations 7–10 the share of Chrysophytes and Prymnesiophyceae pigments was relatively larger. The share of Chrysophyceae was particularly large at the DCM, even dominating the phytoplankton community biomass at Stations 15–23 (Table S1). Diatoms (Bacillariophyceae) contributed substantially in the surface waters of Station 8, up to 21 % of total Chl *a*.

3.2 Diazotroph enumeration

The diazotroph cyanobacteria were divided into five categories: three of them are symbionts, i.e., with the diatoms *Rhizosolenia* cf. *clevei*, *Hemiaulus hauckii* and *Guinardia cylindrus* DDAs, and two are non-symbionts, i.e., *Trichodesmium* colonies (> 10 trichomes organized into a coherent structure) and free *Trichodesmium* trichomes (Fig. 4a–e, Table S3). Total DDA abundance was low (0–21 combined DDA *Richelia* trichomes L⁻¹) at the oceanic stations (Stations 1–6). *Hemiaulus* DDA abundance was greatest at Station 8 (ca. 4.0×10^3 trichomes L⁻¹) with a secondary maximum at Station 17 (0.8×10^3 trichomes L⁻¹), both in the surface (< 5 m) waters. *Rhizosolenia* DDA abundance was lower than *Hemiaulus* DDA abundance at Station 7 (*Rhizosolenia* DDA ca. 60 trichomes L⁻¹) and at Stations 15 and 16 (*Rhizosolenia* DDA, ca. 80 trichomes L⁻¹). *Rhizosolenia* DDAs were not observed below 31.6 salinity (Fig. 4a). *Hemiaulus* DDA were observed down to 27.1–27.6 salinity at ~ 80–100 trichomes L⁻¹ (Fig. 4b). Free *Trichodesmium* trichomes were broadly distributed (Fig. 4d) and often occurred across a wide depth range, down to 75 m at Station 17. *Trichodesmium* colonies were seen sporadically and with distributions dominated by two sampling points (Station 6, 32 m and Station 21, 60 m) where colony abundance > 25 colonies L⁻¹. A single observation of colonies at depth under the low-salinity plume generated contour lines suggesting a generalized presence at depth. However, removal of this observation (Station 14, 61 m) removed this trend and resulted in distinct separation of the colony distributions, i.e., two areas of increased biomass associated with salinity gradients at the edge of the river plume.

3.3 Heterocyst glycolipids in suspended particulate matter

We analyzed heterocyst glycolipids (HG_s) in SPM from along the cruise transect collected at the surface, bottom wind mixed layer (BWML) and the DCM. Two long-chain C₅ HG_s were detected in the SPM, i.e., 1-(O-ribose)-3,27,29-triacontanetriol and 1-(O-ribose)-3,29,31-dotriacontanetriol (C₅ HG₃₀ and C₅ HG₃₂ triol, respectively, Fig. 1). C₅ HG₃₂ triol represented on average 98 ± 4 % of the summed abundance of the two HG_s. Previous studies of C₅ HG_s have identified 1-(O-ribose)-3,29-triacontanediol (C₅ HG₃₀ diol,

Fig. 1) in both cultures and environmental samples (Bale et al., 2015; Schouten et al., 2013), but these were not seen in the SPM or surface sediment analyzed in this study.

The concentrations of the two C₅ HG_s were highest in the surface waters of Station 8 and showed a second local maxima at Station 16 (Table 1 and Fig. 4f). The surface concentration of the dominant HG, i.e., C₅ HG₃₀ triol, ranged between 0 and 4800 pg L⁻¹. The range in concentration was 50-fold lower at the DCM (0–200 pg L⁻¹, Table S2). The three samples from 200 m depth showed lowest concentrations, ranging between 20.6 and 127 pg L⁻¹. Overall, the C₅ HG₃₀ triol was consistently present in the higher concentration of the two (Fig. 4f). The minor HG, i.e., C₅ HG₃₂ triol, ranged between 0 and 10 % of their summed abundance at the surface and BWML, was between 0 and 5 % at the DCM and 0 and 17 % at 200 m (see Fig. 4f contour lines and Table S2).

HG_s with a C₆ sugar head group were not detected in any SPM samples with the exception of one sample, taken at Station 20a from the DCM (65 m). 1-(O-hexose)-3,25-hexacosanediol (C₆ HG₂₆ diol, Fig. 1) and 1-(O-hexose)-3-keto-25-hexacosanol (C₆ HG₂₆ keto-ol) were confidently identified from their [M+H]⁺ accurate mass (*m/z* 577.4674 and 575.4517, respectively) and their fragmentation patterns, which followed published reports (Bauersachs et al., 2009b). C₆ HG₂₆ diol and C₆ HG₂₆ keto-ol were present at concentrations of 0.3 and 0.4 ng L⁻¹, respectively (data not shown), both ~ 10 times higher than the concentration of the C₅ HG₃₀ triol in this sample (Table 1).

At Station 10, besides SPM samples collected on 0.7 μm GF/Fs, SPM samples were also collected at depths down to 3000 m using 0.3 μm GF75 filters (Table 2). As with the 0.7 μm SPM samples at station 10, C₅ HG₃₀ triol was consistently present in higher concentration than C₅ HG₃₂ triol (which represented on average only 1.4 ± 0.7 % of their summed abundance). The concentrations and depth trends (to 200 m) of the two C₅ HG_s did not differ between the 0.3 and 0.7 μm filter SPM samples (Fig. 5). For both the 0.3 μm samples and the 0.7 μm samples, the summed abundance of C₅ HG₃₀ triol and C₅ HG₃₂ triol was highest at 200 m, 108 pg L⁻¹. In the 0.3 μm samples, both concentrations decreased below 200 m, although both C₅ HG_s remained detectable at 3000 m depth.

3.4 Heterocyst glycolipids and bulk properties in surface sediment

As with the SPM, C₅ HG₃₀ triol and C₅ HG₃₂ triol were detected in the surface sediment of 17 stations (Table 1). Here C₅ HG₃₀ triol was also consistently present in the higher concentration of the two (C₅ HG₃₂ triol represented on average 9.4 ± 3.0 % of their summed abundance). The C₅ HG₃₀ diol was not detected in any surface sediment, like the SPM samples. HG_s with a C₆ sugar head group were also not detected in any surface sediment. In the sediment underlying the high-salinity open ocean stations (1, 3, 5)

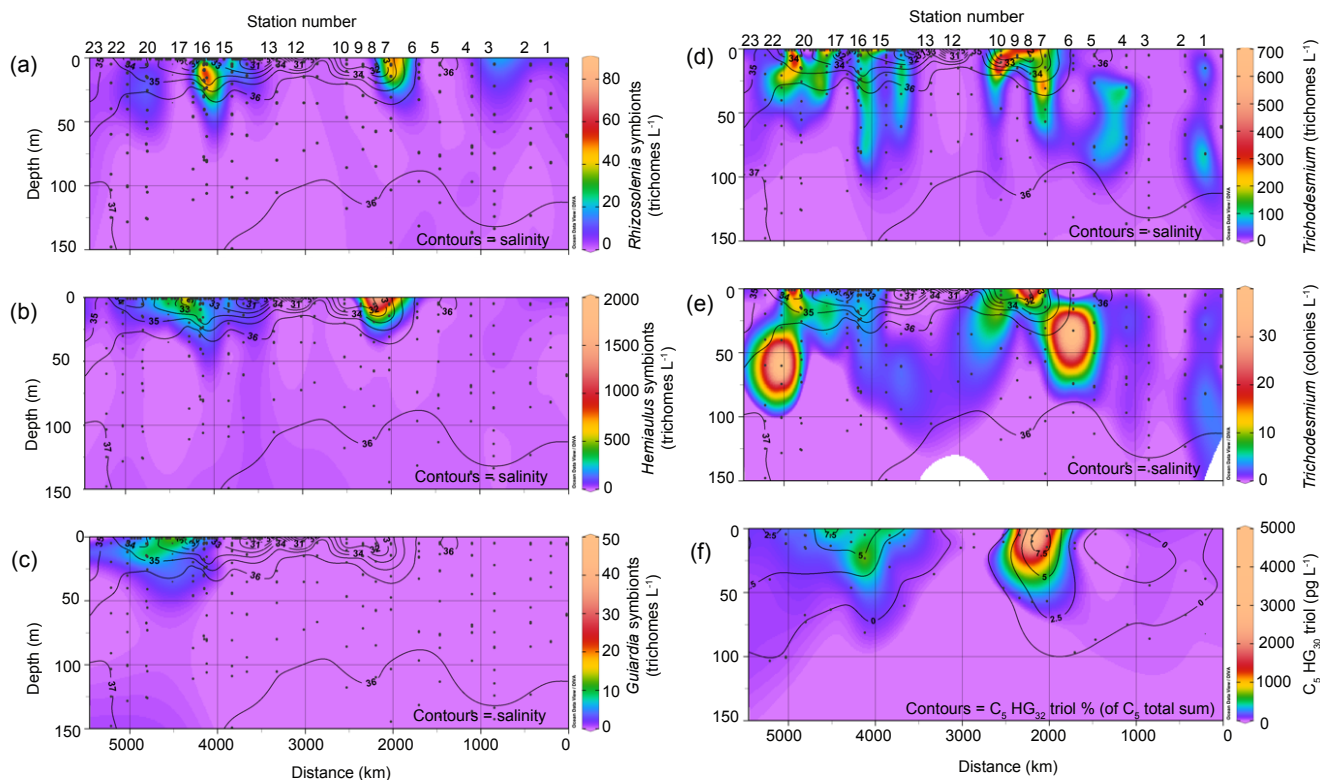


Figure 4. Diazotroph abundance along the cruise track. Color scales show (a) *Rhizosolenia* symbionts (trichomes L^{-1}), (b) *Hemiaulus* symbionts (trichomes L^{-1}), (c) *Guillardia* symbionts (trichomes L^{-1}), (d) *Trichodesmium* (free trichomes L^{-1}) and (e) *Trichodesmium* (colonies L^{-1}), while contour lines show salinity (a–e). (f) Color scale shows concentration of C_5 HG₃₀ triol ($pg L^{-1}$) while contour lines show C_5 HG₃₂ triol % (of C_5 total sum). Station numbers noted above plots, distance along transect from the Cabo Verde islands below. Dots in (a–c) indicate sampling depth for the salinity contours. Dots in (a–e) indicate sampling depth for the salinity contours. Dots in (f) indicate sampling depth for HG lipids.

the summed abundance of the two C_5 HGs was low (2.0 – $3.7 ng g^{-1}$, Table 1). It was high at Stations 7 and 8 (10.6 and $16.3 ng g^{-1}$), while Stations 9–17 contained mid-range concentrations (5.2 – $14.8 ng g^{-1}$), with the exception of the two coastal-shelf stations (11 and 12) where the concentration was at its lowest (0.2 and $0.3 ng g^{-1}$). At the final four stations (20a, 21a, 22 and 23) the summed abundance returned to high levels (11.2 – $19.0 ng g^{-1}$). For context, the TOC was relatively stable between Stations 1 and 10 (avg. $0.6 \pm 0.1 \%$, $n = 7$) and then low at Station 11 and 12 (avg. $0.2 \pm 0.1 \%$). Station 13 exhibited the highest TOC of all the stations ($1.2 \pm 0.0 \%$), and TOC decreased steadily at all stations thereafter, and was $0.6 \pm 0.0 \%$ at Station 23.

4 Discussion

4.1 Heterocyst glycolipids and DDAs in the water column

The Amazon plume has been extensively documented to support high numbers of the diatom–diazotroph associations

(DDA) such as *Hemiaulus hauckii*–*Richelia intracellularis* and *Rhizosolenia clevei*–*Richelia intracellularis* (Carpenter et al., 1999; Foster et al., 2007; Goes et al., 2014; Subramaniam et al., 2008; Weber et al., 2017). Our study took place outside the high Amazon flow period and the Chl concentrations and DDA counts encountered on this cruise did not reach the values seen in “bloom conditions” described during previous studies in the region (Carpenter et al., 1999; Subramaniam et al., 2008). However, the DDA counts in certain stations were up to 3 orders of magnitude higher than surrounding waters and comparable to the open ocean DDA blooms seen in the North Pacific Gyre (Villareal et al., 2011, 2012). These strong gradients permitted investigation of relationships between DDA and HG distributions.

The concentrations of the C_5 HG₃₀ triol and C_5 HG₃₂ triol were correlated with the cell counts of different diazotrophs. The concentrations of both the C_5 HGs (C_5 HG₃₀ triol and C_5 HG₃₂ triol) exhibited the most significant positive Pearson correlation with the number of *Hemiaulus* symbionts ($p \leq 0.001$, $r = 0.79$ and 0.78 , respectively; $n = 54$). While these long-chain C_5 heterocyst glycolipids (HGs) have been found in cultures of DDAs (Bale et al., 2015; Schouten et al., 2013),

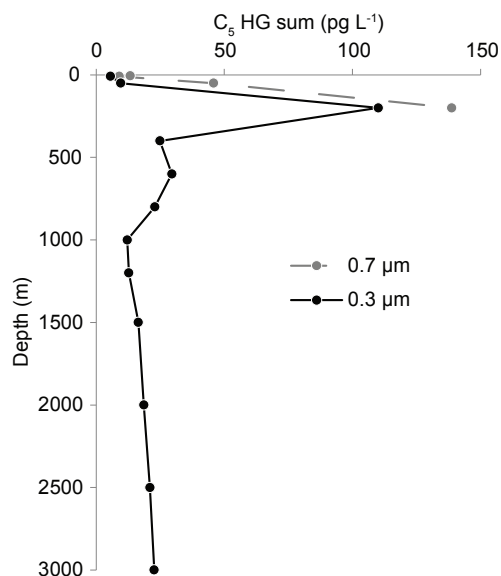


Figure 5. Station 10: down column profile of C₅ HG sum (C₅ HG₃₀ triol + C₅ HG₃₂ triol, pg L⁻¹) from 0.7 μm GF/F filters (grey dashed line) and 0.3 μm GF75 filters (solid black line).

our study of the tropical North Atlantic provides for the first time, to the best of our knowledge, environmental evidence that long-chain C₅ HGs track the abundance and distribution of DDAs.

Interestingly, there was no significant correlation found between the number of *Rhizosolenia* symbionts and the concentration of the C₅ HGs (C₅ HG₃₀ triol: $p = 0.07$, $r = 0.23$; and C₅ HG₃₂ triol: $p = 0.14$, $r = 0.19$), except when the surface and BWML of Station 8 were excluded from the analysis (C₅ HG₃₀ triol: $p \leq 0.001$, $r = 0.88$; and C₅ HG₃₂ triol: $p \leq 0.001$, $r = 0.83$). This difference may in part be due to the lower number of *Rhizosolenia*/*Guinardia* symbionts relative to *Hemiaulus* symbionts (on average *Rhizosolenia* symbionts in this study represented $24 \pm 34\%$ of the sum of *Rhizosolenia* and *Hemiaulus* symbionts), similar to previous findings that *Hemiaulus* dominated over *Rhizosolenia* in the Amazon plume (Foster et al., 2007) and Caribbean region (Villareal, 1994). Furthermore, culture studies have shown that *Rhizosolenia* symbionts contain only trace amounts of C₅ HG₃₀ triol (Bale et al., 2015), whereas this is a dominant HG in *Hemiaulus* symbionts (Schouten et al., 2013). Unfortunately, a unique biomarker for *Rhizosolenia* and *Guinardia* symbionts has not been identified to date (Bale et al., 2015; Schouten et al., 2013). There was also a significant correlation between C₅ HG₃₂ triol (but not C₅ HG₃₀ triol) and the counts of *Guinardia cylindrus* (formerly *Rhizosolenia cylindrus*; $p \leq 0.03$, $r = 0.49$, $n = 21$). This was the only species for which there was a correlation with C₅ HG₃₂ triol but not C₅ HG₃₀ triol. This DDA has not been cultured and nothing is known about the heterocyst lipid composition of this

species. These results suggest C₅ HG₃₀ triol may be synthesized by this species.

At approximately half of the sampling points, glycolipids could be detected in SPM where no DDAs were observed by microscopy. This difference may be the result of the difference in total sampling volumes between the two methods which led to a higher probability that the lipid samples would contain symbiont chains than the microscopy samples. In addition, microscopic examinations may have missed heterocysts that were incorporated into unrecognizable masses in aggregates, whereas UHPLC-HRMS may have still detected the associated HGs. Indeed, copepod grazing in the plume (Conroy et al., 2016) will repackage *Richelia* trichomes, and little is known of the effects of gut passage on heterocyst and HG integrity. It should also be noted that because sampling for diazotroph enumeration and for lipid analysis occurred via different methods, there was a time offset of ≤ 5 h and a depth offset of ≤ 20 m between the two sampling events representing the same water column phenomena (surface, BWML and DCM).

Unexpectedly, a significant correlation was also found for C₅ HG₃₀ triol and C₅ HG₃₂ triol and the number of *Trichodesmium* colonies ($p \leq 0.001$, $r = 0.68$ and 0.67 , $n = 54$), and for C₅ HG₃₀ triol and the number of *Trichodesmium* filaments ($p \leq 0.05$, $r = 0.30$, $n = 54$). These correlations could be coincidental as C₅ HG-producing organisms have not been described in association with *Trichodesmium*, nor would *Trichodesmium* be expected to produce HGs itself as it does not use heterocysts to fix nitrogen. A recent study in the North Pacific Subtropical Gyre found that *Trichodesmium* colonies were harboring an endobiotic heterocystous cyanobacteria of the genus *Calothrix* (Momper et al., 2015). However, analyses of the HG content of both freshwater and marine *Calothrix* cultures have to date only revealed the presence of C₆ HGs, not C₅ HGs (Bauersachs et al., 2009a; Schouten et al., 2013; Wörmer et al., 2012). Furthermore, no heterocystous cyanobacteria were observed in *Trichodesmium* from the Caribbean (Borstad, 1978) or southwest Sargasso Sea (Siddiqui et al., 1992). *Trichodesmium* is reported to have a physiological differentiated cell (diazocyte) that permits N₂ fixation in an oxygenated colony or trichome, and which lacks the thickened cell envelope of heterocysts where HGs are localized (Sandh et al., 2012).

While elevated HGs were statistically more associated with the DDA blooms than either free or colonial *Trichodesmium*, there was frequently a co-occurrence of *Trichodesmium* with the DDA taxa (Fig. 4) which could also contribute to the unexpected correlation. The *Trichodesmium* distribution appears to contrast with the findings of Foster et al. (2007), Goes et al. (2014) and Subramaniam et al. (2008), who all concluded that changing nutrient availability as reflected in the salinity gradient along the Amazon River plume led to zonation of the diazotroph community. However, their data were examining more pronounced DDA cell abundance concentrations under much higher Amazon

plume flow conditions. The broader features of our observations, i.e., a low-salinity region with higher nutrient concentrations and few diazotrophs transitioning to strong diazotroph gradients in the salinity gradient to oceanic conditions, are in concordance with their observations.

Visual examination of the correlations between the C₅ HG concentration and the four major diazotrophs groups (*Hemiaulus* symbionts, *Rhizosolenia* symbionts, *Trichodesmium* colonies and *Trichodesmium* filaments) showed a clear outlier in the *Hemiaulus* symbiont regression curve, i.e., Station 8 at 10 m water depth (Fig. S2a). As the DDAs and *Trichodesmium* are all surface dwellers (upper 5 m) we postulated that this depth contained detrital HGs not reflecting living heterocystous cyanobacteria. Hence we also plotted the four regressions for only surface data ($n = 19$, Fig. S2b). The correlation between the number of *Hemiaulus* symbionts and the C₅ HG concentration became substantially stronger ($p < 0.001$, $r^2 = 0.97$), as did that of the *Trichodesmium* colonies ($p < 0.001$, $r^2 = 0.94$). However, closer examination showed that one station, again Station 8, with unusually high levels of both *Hemiaulus* symbionts and *Trichodesmium* colonies (Station 8) was responsible for these high correlation coefficients. Removal of Station 8 from the regressions ($n = 18$, Fig. S2c) revealed that the number of *Hemiaulus* symbionts still correlated with the C₅ HG concentration ($p < 0.001$, $r^2 = 0.67$) but the correlation with *Trichodesmium* colonies had disappeared ($p = 0.47$, $r^2 = 0.03$). Interestingly in this third sample subset there was also a significant correlation between the number of *Rhizosolenia* symbionts and the C₅ HG concentration ($p < 0.001$, $r^2 = 0.56$).

Two C₆ HGs, generally associated with free-living heterocyst-forming cyanobacteria from freshwater or brackish environments (Bale et al., 2015, 2016; Bauersachs et al., 2009b, 2010, 2011; Bühring et al., 2014; Wörmer et al., 2012), were identified only in the DCM of Station 20a (C₆ HG₂₆ diol and C₆ HG₂₆ keto-ol). Whereas in this study the two C₆ HGs were found at a similar concentration to each other, previous studies have reported that C₆ HG₂₆ keto-ol was detected as a minor component relative to the more abundant C₆ HG₂₆ diol (Bale et al., 2015, 2016; Bauersachs et al., 2009a, b, 2011; Schouten et al., 2013; Wörmer et al., 2012). An earlier study executed nearer to the mouth of the Amazon river detected trace levels of C₆ HG₂₆ diol (but not C₆ HG₂₆ keto-ol) in surface sediments (Bale et al., 2015). In contrast, both C₆ HG₂₆ diol and C₆ HG₂₆ keto-ol were recorded in freshwater Amazon River water and floodplain lake sediment.

There are reports of cyanobacterial species in cohabitation with other planktonic organisms such as the floating macroalgae *Sargassum* (Carpenter, 1972; Hanson, 1977; Philips et al., 1986) and *Trichodesmium* (Momper et al., 2015). While the HG content of the cyanobacteria in these co-habitations has not been investigated, these cyanobacteria are in the same families as known C₆ HG producers (Bauersachs et al., 2009a; Schouten et al., 2013; Wörmer et al., 2012). *Tri-*

chodesmium was not detected by microscopy at this sampling point; however as stated above, there is an apparent difference regarding the limit of detection between counting by microscopy and lipid analysis by UHPLC-HRMS. Floating “fields” of *Sargassum* were regularly encountered during the research cruise, with the maximum observations occurring around Station 16. Further work on the HG composition of the cyanobacteria found in these cohabitations would be necessary to draw conclusions as to whether they contributed to the source of the two C₆ HGs detected at this sampling point.

4.2 C₅ heterocyst glycolipids below the DCM

While the concentration of the C₅ HGs was generally highest within the mixed layer (ML; see Fig. 4f), Station 10 exhibited an increase in C₅ HG concentration with depth with C₅ HGs in both the 0.3 and 0.7 μm samples increasing with depth to a maximum at 200 m (Fig. 5). The two size fraction profiles were carried out approximately 12 h apart and suggest that the HG maxima at 200 m was a feature for at least this period of time. Station 9 was the only other station where the C₅ HG concentration (0.7 μm) at the DCM was higher than in the ML (see Table S1). Foster et al. (2007) reported that DDAs are high in the ML but can increase below the ML down to at least 100 m. Sediment trap studies in the North Pacific and tropical North Atlantic ocean have found significant contributions by DDAs to the vertically exported particulate organic carbon (Karl et al., 2012; Scharek et al., 1999; Subramaniam et al., 2008). While our study did not utilize sediment traps to collect sinking particles, a proportion of the matter collected by in situ filtration is probably sinking rather than suspended (Abramson et al., 2010). C₅ HGs have been found in surface sediment at depths up to 3000 m underlying our water column sampling points (this study and Bale et al., 2015), supporting the hypothesis that DDAs are effectively transported in this environment from the water column to the sediment. These sinking particles could be due to bloom termination and aggregation or sinking of zooplankton fecal pellets.

4.3 C₅ heterocyst glycolipids in surface sediment

As was found in a previous study concentrating on a smaller area close to the mouth of the Amazon (Bale et al., 2015), the presence of a similar distribution of C₅ HGs in SPM and surface sediment indicates that HG producers sink, probably enhanced by the mineral ballast as well as matrix protection provided by the association with diatom silica skeletons. The total C₅ HG concentration in surface sediments was more spatially homogenous than the distribution in the SPM (Table 1). Other than the two stations very close to the coast (where currents were high and the TOC content was at its lowest), the HGs were detected in comparably high levels from Station 7 onwards. This reflects the wide spatial range of the HG producers through an “integrated” multi-decadal

record of their deposition. Each year between June and January, the Amazon plume is retroflected offshore, across the Atlantic towards Africa due to the actions of the North Brazil Current and the North Equatorial Countercurrent, which may account for the presence of the C₅ HGs in the surface sediments of Stations 1–10. The rest of the year the Amazon water flows northwestward towards the Caribbean Sea as the countercurrent and the retroflection weaken or vanish (Muller-Karger et al., 1988), in turn accounting for the C₅ HGs in the surface sediments of Stations 13–23.

5 Conclusions

Long-chain C₅ HGs were detected in the water column of the tropical North Atlantic and their concentrations correlated strongly with DDAs. Furthermore, the HGs tracked the movement of the DDAs to the surface sediments in areas known to be impacted by high seasonal DDA input (under the Amazon plume) whereas the HG concentration in sediment farther away from plume was low. We conclude that long-chain C₅ HGs provide a robust, reliable method for detecting DDAs in the marine environment. The apparent stability and specificity of C₅ HGs mean that they have high potential for use in future work examining the presence and N cycling role of DDAs in the past.

Data availability. Data are archived and available at <https://doi.org/10.1594/PANGAEA.886399> (Bale et al., 2018).

The Supplement related to this article is available online at <https://doi.org/10.5194/bg-15-1229-2018-supplement>.

Competing interests. The authors declare that they have no conflict of interest.

Acknowledgements. We thank the captains and crew of the R/V *Pelagia* for their support during the cruise. We thank Yvo Witte and Sander Asjes for technical support onboard and Sharyn Ossebaar for nutrient sample collection and analysis. We thank colleagues from the MMB lab (NIOZ) for assistance with sample collection and processing. We also thank Steven de Vries for C₆ HG data analysis. The work of Nicole J. Bale is supported by the Netherlands Organisation for Scientific Research (NWO) through grant 822.01.017 to Stefan Schouten. Stefan Schouten was funded by the European Research Council (ERC) under the European Union's Seventh Framework Programme (FP7/2007-2013) ERC grant agreement 339206. Stefan Schouten and Jaap S. Sinninghe Damsté receive financial support from the Netherlands Earth System Science Centre (NESSC).

Edited by: Silvio Pantoja

Reviewed by: two anonymous referees

References

- Abramson, L., Lee, C., Liu, Z., Wakeham, S. G., and Szlosek, J.: Exchange between suspended and sinking particles in the north-west Mediterranean as inferred from the organic composition of in situ pump and sediment trap samples, *Limnol. Oceanogr.*, 55, 725–739, <https://doi.org/10.4319/lo.2010.55.2.0725>, 2010.
- Abreu-Grobois, F. A., Billyard, T. C., and Walton, T. J.: Biosynthesis of heterocyst glycolipids of *Anabaena cylindrica*, *Phytochemistry*, 16, 351–354, [https://doi.org/10.1016/0031-9422\(77\)80063-0](https://doi.org/10.1016/0031-9422(77)80063-0), 1977.
- Bale, N., de Vries, S., Hopmans, E. C., Sinninghe Damsté, J. S., and Schouten, S.: A method for quantifying heterocyst glycolipids in biomass and sediments, *Org. Geochem.*, 110, 33–35, <https://doi.org/10.1016/j.orggeochem.2017.04.010>, 2017.
- Bale, N. J., Villanueva, L., Hopmans, E. C., Schouten, S., and Sinninghe Damsté, J. S.: Different seasonality of pelagic and benthic Thaumarchaeota in the North Sea, *Biogeosciences*, 10, 7195–7206, <https://doi.org/10.5194/bg-10-7195-2013>, 2013.
- Bale, N. J., Hopmans, E. C., Zell, C., Sobrinho, R. L., Kim, J.-H., Sinninghe Damsté, J. S., Villareal, T. A., and Schouten, S.: Long chain glycolipids with pentose head groups as biomarkers for marine endosymbiotic heterocystous cyanobacteria, *Org. Geochem.*, 81, 1–7, <https://doi.org/10.1016/j.orggeochem.2015.01.004>, 2015.
- Bale, N. J., Hopmans, E. C., Schoon, P. L., de Kluijver, A., Downing, J. A., Middelburg, J. J., Sinninghe Damsté, J. S., and Schouten, S.: Impact of trophic state on the distribution of intact polar lipids in surface waters of lakes, *Limnol. Oceanogr.*, 61, 1065–1077, <https://doi.org/10.1002/lno.10274>, 2016.
- Bale, N. J., Villareal, T. A., Hopmans, E. C., Brussaard, C. P. D., Besseling, M., Dorhout, D. J. C., Sinninghe Damsté, J. S., and Schouten, S.: C₅ glycolipids of heterocystous cyanobacteria track symbiont abundance in the diatom *Hemiaulus hauckii* across the tropical North Atlantic, *PANGAEA*, <https://doi.org/10.1594/PANGAEA.886399>, 2018.
- Bauersachs, T., Compaore, J., Hopmans, E. C., Stal, L. J., Schouten, S., and Sinninghe Damsté, J. S.: Distribution of heterocyst glycolipids in cyanobacteria, *Phytochemistry*, 70(17–18), 2034–2039, <https://doi.org/10.1016/j.phytochem.2009.08.014>, 2009a.
- Bauersachs, T., Hopmans, E. C., Compaore, J., Stal, L. J., Schouten, S., and Sinninghe Damsté, J. S.: Rapid analysis of long-chain glycolipids in heterocystous cyanobacteria using high-performance liquid chromatography coupled to electrospray ionization tandem mass spectrometry, *Rapid Commun. Mass Sp.*, 23, 1387–1394, <https://doi.org/10.1002/rcm.4009>, 2009b.
- Bauersachs, T., Speelman, E. N., Hopmans, E. C., Reichart, G.-J., Schouten, S., and Sinninghe Damsté, J. S.: Fossilized glycolipids reveal past oceanic N₂ fixation by heterocystous cyanobacteria, *P. Natl. Acad. Sci. USA*, 107, 19190–19194, <https://doi.org/10.1073/pnas.1007526107>, 2010.
- Bauersachs, T., Compaore, J., Severin, I., Hopmans, E. C., Schouten, S., Stal, L. J., and Sinninghe Damsté, J. S.: Diazotrophic microbial community of coastal microbial

- mats of the southern North Sea, *Geobiology*, 9, 349–359, <https://doi.org/10.1111/j.1472-4669.2011.00280.x>, 2011.
- Bauersachs, T., Mudimu, O., Schulz, R., and Schwark, L.: Distribution of long chain heterocyst glycolipids in N₂ fixing cyanobacteria of the order Stigonematales, *Phytochemistry*, 98, 145–150, <https://doi.org/10.1016/j.phytochem.2013.11.007>, 2014.
- Besseling et al.: in preparation, 2018.
- Borstad, G. A.: Some Aspects of the Occurrence and Biology of *Trichodesmium* (Cyanophyta) in the Western Tropical Atlantic near Barbados, West Indies, McGill University, Montreal, 1978.
- Bryce, T. A., Welti, D., Walsby, A. E., and Nichols, B. W.: Monohexoside derivatives of long-chain polyhydroxy alcohols; a novel class of glycolipid specific to heterocystous algae, *Phytochemistry*, 11, 295–302, [https://doi.org/10.1016/S0031-9422\(00\)90006-2](https://doi.org/10.1016/S0031-9422(00)90006-2), 1972.
- Buddrick, O., Jones, O. A. H., Morrison, P. D., and Small, D. M.: Heptane as a less toxic option than hexane for the separation of vitamin E from food products using normal phase HPLC, *RSC Adv.*, 3, 24063, <https://doi.org/10.1039/c3ra44442b>, 2013.
- Bühning, S. I., Kamp, A., Wörmer, L., Ho, S., and Hinrichs, K.-U.: Functional structure of laminated microbial sediments from a supratidal sandy beach of the German Wadden Sea (St. Peter-Ording), *J. Sea Res.*, 85, 463–473, <https://doi.org/10.1016/j.seares.2013.08.001>, 2014.
- Carelli, V., Franceschini, F., Venturi, S., Barboni, P., Savini, G., Barbieri, G., Pirro, E., La Morgia, C., Valentino, M. L., Zanardi, F., Violante, F. S., and Mattioli, S.: Grand rounds: Could occupational exposure to n-hexane and other solvents precipitate visual failure in Leber hereditary optic neuropathy?, *Environ. Health Persp.*, 115, 113–115, <https://doi.org/10.1289/ehp.9245>, 2007.
- Carpenter, E. J.: Nitrogen fixation by a blue-green epiphyte on pelagic *Sargassum*, *Science*, 178, 1207–1209, <https://doi.org/10.1126/science.178.4066.1207>, 1972.
- Carpenter, E. J., Montoya, J. P., Burns, J., Mulholland, M. R., Subramaniam, A., and Capone, D. G.: Extensive bloom of a N₂-fixing diatom/cyanobacterial association in the tropical Atlantic Ocean, *Mar. Ecol.-Prog. Ser.*, 185, 273–283, <https://doi.org/10.3354/meps185273>, 1999.
- Conroy, B. J., Steinberg, D. K., Stukel, M. R., Goes, J. I., and Coles, V. J.: Meso- and microzooplankton grazing in the Amazon River plume and western tropical North Atlantic, *Limnol. Oceanogr.*, 61, 825–840, <https://doi.org/10.1002/lno.10261>, 2016.
- Daughtrey, W., Newton, P., Rhoden, R., Kirwin, C., Haddock, L., Duffy, J., Keenan, T., Richter, W., and Nicolich, M.: Chronic inhalation carcinogenicity study of commercial hexane solvent in F-344 rats and B6C3F1 mice, *Toxicol. Sci.*, 48, 21–29, <https://doi.org/10.1093/toxsci/48.1.21>, 1999.
- Elliott, M. and McLusky, D. S.: The need for definitions in understanding estuaries, *Estuar. Coast. Shelf Sci.*, 55, 815–827, <https://doi.org/10.1006/ecss.2002.1031>, 2002.
- Foster, R. A. and Zehr, J. P.: Characterization of diatom-cyanobacteria symbioses on the basis of nifH, hetRand 16S rRNA sequences, *Environ. Microbiol.*, 8, 1913–1925, 2006.
- Foster, R. A., Subramaniam, A., Mahaffey, C., Carpenter, E. J., Capone, D. G., and Zehr, J. P.: Influence of the Amazon River plume on distributions of free-living and symbiotic cyanobacteria in the western tropical north Atlantic Ocean, *Limnol. Oceanogr.*, 52, 517–532, 2007.
- Foster, R. A., Kuypers, M. M. M., Vagner, T., Paerl, R. W., Musat, N., and Zehr, J. P.: Nitrogen fixation and transfer in open ocean diatom-cyanobacterial symbioses, *ISME J.*, 5, 1484–1493, <https://doi.org/10.1038/ismej.2011.26>, 2011.
- Gambacorta, A., Soriente, A., Trincone, A., and Sodano, G.: Biosynthesis of the heterocyst glycolipids in the cyanobacterium *Anabaena cylindrica*, *Phytochemistry*, 39, 771–774, [https://doi.org/10.1016/0031-9422\(95\)00007-T](https://doi.org/10.1016/0031-9422(95)00007-T), 1995.
- Gambacorta, A., Pagnotta, E., Romano, I., Sodano, G., and Trincone, A.: Heterocyst glycolipids from nitrogen-fixing cyanobacteria other than Nostocaceae, *Phytochemistry*, 48, 801–805, [https://doi.org/10.1016/S0031-9422\(97\)00954-0](https://doi.org/10.1016/S0031-9422(97)00954-0), 1998.
- Goes, J. I., Gomes, H. do R., Chekalyuk, A. M., Carpenter, E. J., Montoya, J. P., Coles, V. J., Yager, P. L., Berelson, W. M., Capone, D. G., Foster, R. A., Steinberg, D. K., Subramaniam, A., and Hafez, M. A.: Influence of the Amazon River discharge on the biogeography of phytoplankton communities in the western tropical north Atlantic, *Prog. Oceanogr.*, 120, 29–40, <https://doi.org/10.1016/j.pocean.2013.07.010>, 2014.
- Gómez, F., Furuya, K., and Takeda, S.: Distribution of the cyanobacterium *Richelia intracellularis* as an epiphyte of the diatom *Chaetoceros compressus* in the western Pacific Ocean, *J. Plankton Res.*, 27, 323–330, <https://doi.org/10.1093/plankt/fbi007>, 2005.
- Grasshoff, K., Ed.: *Methods of Seawater Analysis*, 2nd ed., Verlag Chemie, Weinheim, 1983.
- Hanson, R. B.: Pelagic *Sargassum* community metabolism: Carbon and nitrogen, *J. Exp. Mar. Biol. Ecol.*, 29, 107–118, [https://doi.org/10.1016/0022-0981\(77\)90042-9](https://doi.org/10.1016/0022-0981(77)90042-9), 1977.
- Hilton, J. A.: Ecology and Evolution of Diatom-associated Cyanobacteria through Genetic Analyses, PhD thesis, University of California, Santa Cruz, USA, 2014.
- Janson, S., Wouters, J., Bergman, B., and Carpenter, E. J.: Host specificity in the *Richelia*-diatom symbioses revealed by hetR gene sequence analyses, *Environ. Microbiol.*, 1, 431–438, 1999.
- Karl, D., Letelier, R., Tupas, L., Dore, J., Christian, J., and Hebel, D.: The role of nitrogen fixation in biogeochemical cycling in the subtropical North Pacific Ocean, *Nature*, 388, 533–538, <https://doi.org/10.1038/41474>, 1997.
- Karl, D. M., Church, M. J., Dore, J. E., Letelier, R. M., and Mahaffey, C.: Predictable and efficient carbon sequestration in the North Pacific Ocean supported by symbiotic nitrogen fixation, *P. Natl. Acad. Sci. USA*, 109, 1842–1849, <https://doi.org/10.1073/pnas.1120312109>, 2012.
- Lee, K., Karl, D. M., Wanninkhof, R., and Zhang, J. Z.: Global estimates of net carbon production in the nitrate-depleted tropical and subtropical oceans, *Geophys. Res. Lett.*, 29, 13-1–13-4, <https://doi.org/10.1029/2001GL014198>, 2002.
- Luo, Y.-W., Doney, S. C., Anderson, L. A., Benavides, M., Berman-Frank, I., Bode, A., Bonnet, S., Boström, K. H., Böttjer, D., Capone, D. G., Carpenter, E. J., Chen, Y. L., Church, M. J., Dore, J. E., Falcón, L. I., Fernández, A., Foster, R. A., Furuya, K., Gómez, F., Gundersen, K., Hynes, A. M., Karl, D. M., Kitajima, S., Langlois, R. J., LaRoche, J., Letelier, R. M., Marañón, E., McGillicuddy Jr., D. J., Moisander, P. H., Moore, C. M., Mouriño-Carballido, B., Mulholland, M. R., Needoba, J. A., Orcutt, K. M., Poulton, A. J., Rahav, E., Raimbault, P., Rees, A. P., Riemann, L., Shiozaki, T., Subramaniam, A., Tyrrell, T., Turk-Kubo, K. A., Varela, M., Villareal, T. A., Webb, E. A.,

- White, A. E., Wu, J., and Zehr, J. P.: Database of diazotrophs in global ocean: abundance, biomass and nitrogen fixation rates, *Earth Syst. Sci. Data*, 4, 47–73, <https://doi.org/10.5194/essd-4-47-2012>, 2012.
- Mackey, M. D., Mackey, D. J., Higgins, H. W., and Wright, S. W.: CHEMTAX – a program for estimating class abundances from chemical markers: application to HPLC measurements of phytoplankton, *Mar. Ecol.-Prog. Ser.*, 144, 265–283, <https://doi.org/10.3354/meps144265>, 1996.
- Momper, L. M., Reese, B. K., Carvalho, G., Lee, P., and Webb, E. A.: A novel cohabitation between two diazotrophic cyanobacteria in the oligotrophic ocean, *ISME J.*, 9, 882–893, <https://doi.org/10.1038/ismej.2014.186>, 2015.
- Moore, E. K., Hopmans, E. C., Rijpstra, W. I. C., Villanueva, L., Dedysh, S. N., Kulichevskaya, I. S., Wienk, H., Schoutsen, F., and Sinninghe Damsté, J. S.: Novel mono-, di-, and trimethylornithine membrane lipids in northern wetland Planctomycetes, *Appl. Environ. Microb.*, 79, 6874–6884, <https://doi.org/10.1128/AEM.02169-13>, 2013.
- Muller-Karger, F. E., McClain, C. R., and Richardson, P. L.: The dispersal of the Amazon's water, *Nature*, 333, 56–59, <https://doi.org/10.1038/333056a0>, 1988.
- Murphy, J. and Riley, J. P.: A modified single solution method for the determination of phosphate in natural waters, *Anal. Chim. Acta*, 27, 31–36, [https://doi.org/10.1016/S0003-2670\(00\)88444-5](https://doi.org/10.1016/S0003-2670(00)88444-5), 1962.
- Nichols, B. W. and Wood, B. J. B.: New glycolipid specific to nitrogen-fixing blue-green algae, *Nature*, 217, 767–768, <https://doi.org/10.1038/217767a0>, 1968.
- Phlips, E. J., Willis, M., and Verchick, A.: Aspects of nitrogen fixation in *Sargassum* communities off the coast of Florida, *J. Exp. Mar. Biol. Ecol.*, 102, 99–119, [https://doi.org/10.1016/0022-0981\(86\)90170-X](https://doi.org/10.1016/0022-0981(86)90170-X), 1986.
- Riegman, R. and Kraay, G. W.: Phytoplankton community structure derived from HPLC analysis of pigments in the Faroe-Shetland Channel during summer 1999: the distribution of taxonomic groups in relation to physical/chemical conditions in the photic zone, *J. Plankton Res.*, 23, 191–205, <https://doi.org/10.1093/plankt/23.2.191>, 2001.
- Rippka, R., Deruelles, J., Waterbury, J., Herdman, M., and Stanier, R.: Generic assignments, strain histories and properties of pure cultures of cyanobacteria, *J. Gen. Microbiol.*, 111, 1–61, 1979.
- Sandh, G., Xu, L., and Bergman, B.: Diazocyte development in the marine diazotrophic cyanobacterium *Trichodesmium*, *Microbiology*, 158, 345–352, <https://doi.org/10.1099/mic.0.051268-0>, 2012.
- Scharek, R., Latasa, M., Karl, D. M., and Bidigare, R. R.: Temporal variations in diatom abundance and downward vertical flux in the oligotrophic North Pacific gyre, *Deep-Sea Res. Pt. I*, 46, 1051–1075, [https://doi.org/10.1016/S0967-0637\(98\)00102-2](https://doi.org/10.1016/S0967-0637(98)00102-2), 1999.
- Schouten, S., Villareal, T. A., Hopmans, E. C., Mets, A., Swanson, K. M., and Sinninghe Damsté, J. S.: Endosymbiotic heterocystous cyanobacteria synthesize different heterocyst glycolipids than free-living heterocystous cyanobacteria, *Phytochemistry*, 85, 115–121, <https://doi.org/10.1016/j.phytochem.2012.09.002>, 2013.
- Siddiqui, P. J. A., Bergman, B., and Carpenter, E. J.: Filamentous cyanobacterial associates of the marine planktonic cyanobacterium *Trichodesmium*, *Phycologia*, 31, 326–337, <https://doi.org/10.2216/i0031-8884-31-3-4-326.1>, 1992.
- Staal, M., Meysman, F. J. R., and Stal, L. J.: Temperature excludes N₂ fixing heterocystous cyanobacteria in the tropical oceans, *Nature*, 425, 504–507, <https://doi.org/10.1038/nature01999>, 2003.
- Strickland, J. D. H. and Parsons, T. R., Eds.: *A Practical Handbook of Seawater Analysis*, First, Ottawa, 1968.
- Subramaniam, A., Yager, P. L., Carpenter, E. J., Mahaffey, C., Björkman, K., Cooley, S., Kustka, A. B., Montoya, J. P., Sañudo-Wilhelmy, S. A., Shipe, R., and Capone, D. G.: Amazon River enhances diazotrophy and carbon sequestration in the tropical North Atlantic Ocean, *P. Natl. Acad. Sci. USA*, 105, 10460–10465, <https://doi.org/10.1073/pnas.0710279105>, 2008.
- Venrick, E. L.: The distribution and significance of *Richelia intracellularis* Schmidt in the North Pacific Central Gyre, *Limnol. Oceanogr.*, 19, 437–445, <https://doi.org/10.4319/lo.1974.19.3.0437>, 1974.
- Villareal, T.: Nitrogen-fixation by the cyanobacterial symbiont of the diatom genus *Hemiaulus*, *Mar. Ecol.-Prog. Ser.*, 76, 201–204, <https://doi.org/10.3354/meps076201>, 1991.
- Villareal, T. A.: Laboratory culture and preliminary characterization of the nitrogen-fixing *Rhizosolenia-Richelia* symbiosis, *Mar. Ecol.*, 11, 117–132, <https://doi.org/10.1111/j.1439-0485.1990.tb00233.x>, 1990.
- Villareal, T. A.: Widespread occurrence of the *Hemiaulus*-cyanobacteria symbiosis in the southwest North Atlantic Ocean, *B. Mar. Sci.*, 54, 1–7, 1994.
- Villareal, T. A., Adornato, L., Wilson, C., and Schoenbaechler, C. A.: Summer blooms of diatom-diazotroph assemblages and surface chlorophyll in the North Pacific gyre: a disconnect, *J. Geophys. Res.-Oceans*, 116, C03001, <https://doi.org/10.1029/2010JC006268>, 2011.
- Villareal, T. A., Brown, C. G., Brzezinski, M. A., Krause, J. W., and Wilson, C.: Summer diatom blooms in the North Pacific subtropical gyre: 2008–2009, *PLoS One*, 7, e33109, <https://doi.org/10.1371/journal.pone.0033109>, 2012.
- Weber, S. C., Carpenter, E. J., Coles, V. J., Yager, P. L., Goes, J., and Montoya, J. P.: Amazon River influence on nitrogen fixation and export production in the western tropical North Atlantic, *Limnol. Oceanogr.*, 62, 618–631, <https://doi.org/10.1002/lno.10448>, 2017.
- Wolk, C.: Physiology and cytological chemistry of blue-green algae, *Bacteriol. Rev.*, 37, 32–101, 1973.
- Wörmer, L., Cires, S., Velazquez, D., Quesada, A., and Hinrichs, K.-U.: Cyanobacterial heterocyst glycolipids in cultures and environmental samples: diversity and biomarker potential, *Limnol. Oceanogr.*, 57, 1775–1788, <https://doi.org/10.4319/lo.2012.57.6.1775>, 2012.